

## Selective Separation of Am(III)/Eu(III) by the QL-DAPhen Ligand under High Acidity: Extraction, Spectroscopy, and Theoretical Calculations

Shuai Wang,<sup>†</sup> Cui Wang,<sup>†</sup> Xiao-fan Yang, Ji-pan Yu, Wu-qing Tao, Su-liang Yang, Peng Ren, Li-yong Yuan,\* Zhi-fang Chai, and Wei-qun Shi\*



Cite This: *Inorg. Chem.* 2021, 60, 19110–19119



Read Online

ACCESS |



Metrics & More

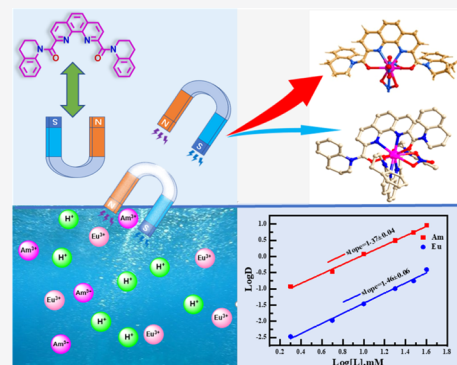


Article Recommendations



Supporting Information

**ABSTRACT:** Although 1,10-phenanthroline-based ligands have recently shown vast opportunities for the separation of trivalent actinides (Ans(III)) from lanthanides (Lns(III)), the optimization and design of the extractant structure based on the phenanthroline framework remain hotspots for further improving the separation. Following the strategy of hard and soft donor atom combination, for the first time, the quinoline group was attached to the 1,10-phenanthroline skeleton, giving a lipophilic ligand, 2,9-diacyl-bis((3,4-dihydroquinoline-1((2H)-yl)-1),10-phenanthroline (QL-DAPhen)), for Am(III)/Eu(III) separation. In the presence of sodium nitrate, the ligand can effectively extract Am(III) over Eu(III) in HNO<sub>3</sub> solution, with the separation factor ( $SF_{Am/Eu}$ ) ranging from 29 to 44. The coordination chemistry of Eu(III) with QL-DAPhen was investigated by slope analysis, NMR titration, UV-vis titration, Fourier transform infrared spectroscopy, electrospray ionization-mass spectrometry, and theoretical calculations. The experimental results unanimously confirm that the ligand forms both 1:1 and 1:2 complexes with Eu(III), and the stability constants ( $\log \beta$ ) of each of the two complexes were obtained. Density functional theory calculations show that the Am–N bonds have more covalent characteristics than the Eu–N bonds in the complexes, which reveals the reason why the ligand preferentially bonds with Am(III). Meanwhile, the thermodynamic analysis reveals that the 1:1 complex is more thermodynamically stable than the 1:2 complex. The findings of this work have laid a solid theoretical foundation for the application of phenanthroline-based ligands in the separation of An(III) from practical systems.



### INTRODUCTION

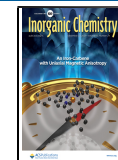
In order to utilize nuclear energy safely and sustainably, the spent nuclear fuel and radioactive waste must be properly handled.<sup>1–3</sup> After the plutonium and uranium recovery process, the high-level liquid waste (HLLW) still contains a certain amount of long-lived small amounts of actinides (Am, Cm, Np, etc.). These nuclides are highly radioactive.<sup>4</sup> In order to reduce the radioactive toxicity and ensure the sustainable development of nuclear energy, it is necessary to develop an advanced nuclear fuel cycle system. Partitioning and transmutation (P&T) strategy is an important alternative technology for the advanced nuclear fuel cycle system. Its purpose is to separate the minor actinides and long-lived fission products in HLLW and use nuclear reactors or accelerators to transmute these long-lived nuclides into short-lived or stable nuclides.<sup>2</sup> Lanthanides from fission products have a large neutron absorption cross section and are toxic to neutrons during the above nuclear reaction, so they must be separated before transmuting. Due to the similarity between trivalent lanthanides (Lns(III)) and actinides (Ans(III)) in terms of ion radius and coordination model, the

separation of Ans(III) and Lns(III) is still considered to be the most challenging task in the field of spent fuel reprocessing.<sup>5,6</sup>

Until now, there is no ideal ligand that satisfies all requirements for the industrial HLLW reprocessing. According to the hard–soft and acid–base (HSAB) theory, Lns(III) are harder than Ans(III).<sup>7,8</sup> Hence, many ligands containing soft N and S donor atoms have been developed in recent years for the separation of Ans(III) over Lns(III).<sup>9–13</sup> S donor ligands, such as Cyanex 301<sup>14–18</sup> and DPAHs,<sup>19</sup> possess an extremely high Ans(III)/Lns(III) separation capability. However, the undesirable acid stability and irradiation resistance of these ligands hinder their practical industrial applications.<sup>20–23</sup> N-Heterocyclic ligands containing only N donors, such as BTPs(2,6-bis(S,6-dialkyl-1,2,4-triazin-3-yl)pyridines),<sup>24</sup> BTBPs(6,6-bis-

Received: September 18, 2021

Published: December 3, 2021



(5,6-dialkyl-1,2,4-triazin-3-yl)-2,2-bipyridine),<sup>25</sup> BTPHens(2,9-bis(1,2,4-triazin-3-yl)-1,10-phenanthroline),<sup>26,27</sup> and BPPhens-(2,9-bis(5-alkyl-1*H*-pyrazol-3-yl)-1,10-phenanthroline),<sup>28</sup> have higher selectivity for Ans(III) than Lns(III). However, these ligands are not consummate. First, the extraction ability of most N-heterocyclic ligands is poor for Ans(III) under high acidity conditions (*e.g.*,  $\text{HNO}_3 > 1 \text{ M}$ ,  $D_{\text{Am}} < 1$ ).<sup>24,25,28</sup> Although some ligands such as CyMe<sub>4</sub>-BTPhen (Figure 1)

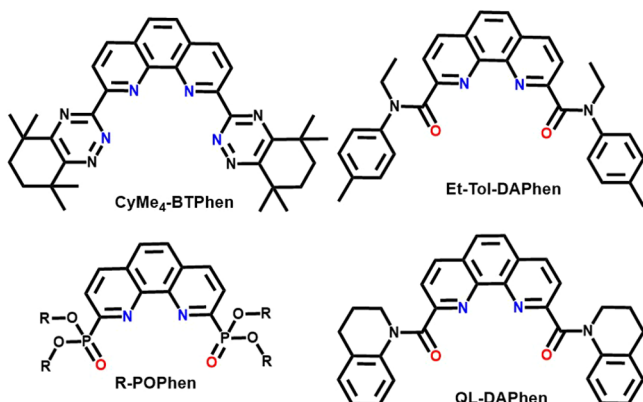


**Figure 1.** Chemical structures of some typical actinide extractants mentioned in this work.

show an extraordinary extraction efficiency for Ans(III) at 0.001–3 M  $\text{HNO}_3$  (*e.g.*,  $D_{\text{Am}} > 10$ ), difficulty in stripping becomes a clear drawback.<sup>26,29</sup> Second, the extraction kinetics of these ligands without a highly preorganized skeleton are always slow; so, it is necessary to introduce phase-transfer agents such as DMDOHEMA(*N,N'*-dimethyl-*N,N'*-dioctylhexyloxyethyl malonamide) and TODGA(*N,N,N',N'*-tetraoctyl diglycolamide).<sup>2,30</sup> Finally, considering the cumbersome synthesis and high cost of these ligands, their application in the actual industry is limited. Thus, there is an urgent need to develop new extractants to overcome the above issues.

Besides the above ligands, 1,10-phenanthroline-derived ligands with hard–soft donors combined in the same molecule also show the potential to separate Ans(III) from Lns(III), which have attracted extensive attention recently.<sup>31–34</sup> For example, a novel tetradentate ligand, *N,N'*-diethyl-*N,N'*-ditolyl-2,9-diamide-1,10-phenanthroline (Et-Tol-DAPhen)<sup>32</sup> (Figure 1), can selectively extract Am(III) ( $D_{\text{Am}} = 6$ ,  $SF_{\text{Am/Eu}} = 67$ ) from excess Eu(III) at 1 M  $\text{HNO}_3$ . Meanwhile, the ligand also has a strong affinity for actinides with higher valence states, such as Th(IV), U(VI), and Pu(IV), so it is expected to be a candidate ligand for group separation of

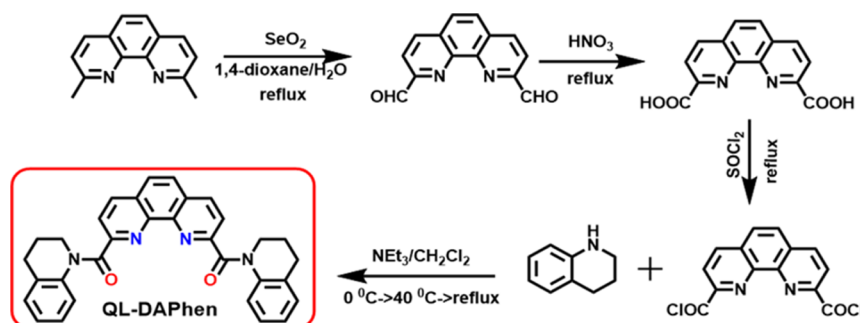
actinides.<sup>35</sup> Subsequently, Xiao *et al.* reported that the phenanthroline-derived phosphonyl ligands, R-POPhen (Figure 1),<sup>36,37</sup> were also efficient for the selective separation of actinides from excess lanthanides. The excellent separation performance of these ligands confirms the feasibility of the soft–hard donor binding strategy for the separation of Ans(III) from Lns(III). However, there are few reports about the 1,10-phenanthroline amide ligands with semirigid large steric hindrance. In order to further explore the influence of the amide accessory group in the 1,10-phenanthroline diamine ligand on the extraction behavior, we reported here a highly preorganized tetradentate diamide ligand constructed with a large quinoline group for the separation of Am(III) from Eu(III). The considerations when we choose the quinoline group as the accessory group of the ligand are as follows: first, the quinoline amide ligand shows the potential of Ln(III)/An(III) separation;<sup>38</sup> second, the quinoline group has a certain rigidity, which is conducive for improving the extraction kinetics; finally, the introduction of this semirigid accessory group will change the species distribution during the extraction, which provides a reference for the design of ligands.

We investigated the extraction performance of the ligand under different extraction conditions and then used a variety of spectral analysis techniques including NMR titration, UV–vis titration, electrospray ionization–mass spectrometry (ESI-MS), Fourier transform infrared (FT-IR) spectroscopy, and so forth to study the complex behavior and extraction mechanism. Moreover, theoretical calculations were used to clarify the intrinsic power of the ligand for the selective extraction of actinides from the differences in electronic properties and bond energies.

## EXPERIMENTAL SECTION

**Chemical Reagents and Methods.** Chemical reagents such as selenium dioxide, 2,9-dimethyl-1,10-phenanthroline, 1,2,3,4-tetrahydroquinoline, 3-nitrotrifluorotoluene,  $\text{Eu}(\text{NO}_3)_3 \cdot 6\text{H}_2\text{O}$ , dichloromethane,  $\text{NaNO}_3$ , tetraethylammonium nitrate, thionyl chloride, triethylamine, and other inorganic or organic reagents were purchased from commercial channels and used without purification.<sup>24</sup> Am (III) in 0.1 M  $\text{HNO}_3$  was provided by China Institute of Atomic Energy. Nuclear magnetic resonance (NMR) spectra were obtained by a Bruker Avance III 500 MHz spectrometer, with tetramethylsilane as the internal solvent resonance reference. FT-IR spectroscopy was measured on a Nicolet Nexus 670 instrument. ESI-MS data were recorded in the form of a positive ion model on the Bruker Amazon SL instrument. The concentration of Eu(III) was obtained on an inductively coupled plasma optical emission spectrometry (ICP-OES Ultima 2, Horiba) system, and the radioactive count of <sup>241</sup>Am was obtained on an  $\alpha$ -liquid flash (FJ414, Beijing Nuclear Instrument Plant).

**Scheme 1.** Synthetic Route of QL-DAPhen



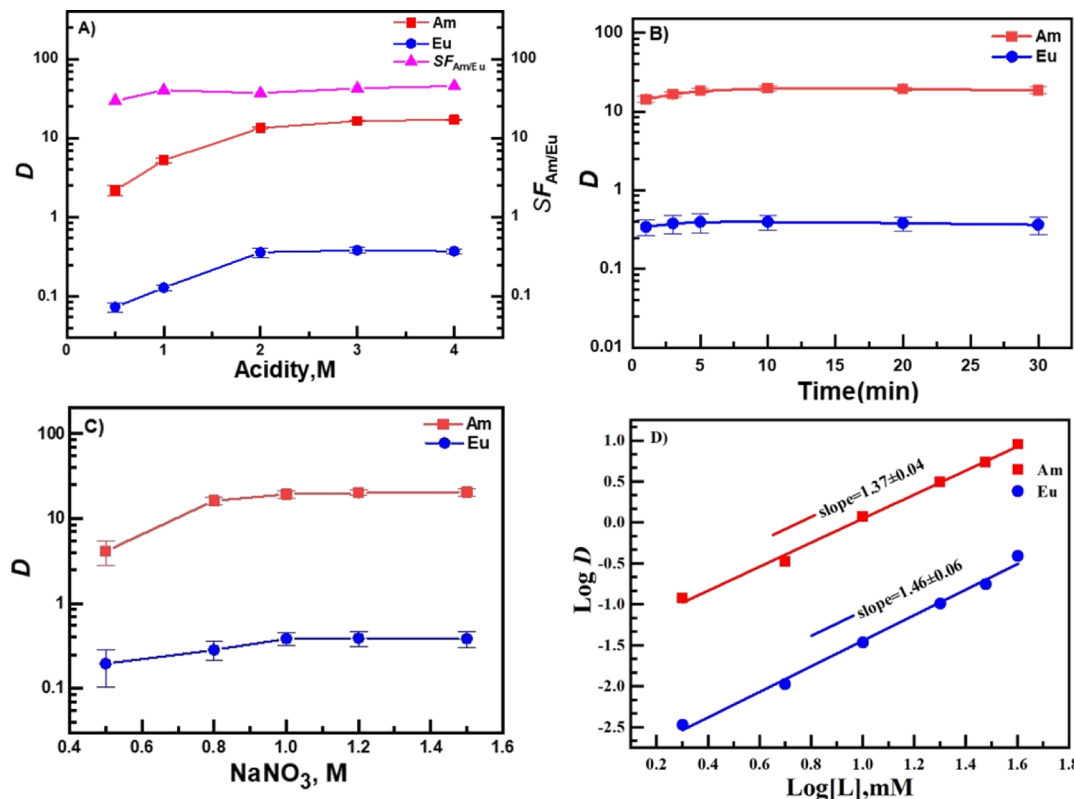


**Figure 2.** Distribution ratios ( $D_M$ ) and separation factor (SF) of Am/Eu by QL-DAPhen in 3-nitrotrifluorotoluene as a function of (A) solution acidity; (B) contact time; (C) concentration of  $\text{NaNO}_3$ ; and (D) concentration of the ligand ([ $\text{HNO}_3$ ] = 0.5–4 M, [contact time] = 0–30 min; [ $\text{NaNO}_3$ ] = 0.5–1.5 M; [ $L$ ] = 2–50 mM).

**Synthesis of the Ligands.** QL-DAPhen was synthesized according to the above route (Scheme 1). 2,9-diformyl-1,10-phenanthroline and 2,9-dicarboxylic acid-1,10-phenanthroline were synthesized according to the procedure reported in the previous works.<sup>39,40</sup>

2,9-Dicarboxylic acid-1,10-phenanthroline (2.02 g, 7.54 mmol) was refluxed with thionyl chloride (50 mL) in an inert atmosphere. After 4 h, the mixture was cooled, and excess thionyl chloride was removed by reduced pressure distillation. When the solvent was completely evaporated, the gray solid was dissolved in dry dichloromethane (50 mL) and cooled in ice water. Subsequently, 1,2,3,4-tetrahydroquinoline (4.01 g, 30.1 mmol) and triethylamine (6.04 g, 59.68 mmol) were added slowly into the mixture. The reaction was continued for 3 h at 40 °C in  $\text{N}_2$  atmosphere. The solvent was removed under reduced pressure, and the residue was purified with silica gel column chromatography (eluent:  $\text{CH}_3\text{OH}/\text{CHCl}_3$  = 1/80) and recrystallized from  $\text{CH}_3\text{OH}/\text{CH}_2\text{Cl}_2$  to yield white powders of ligand L (1.85 g, 41.1%).  $^1\text{H}$  NMR (500 MHz,  $\text{DMSO}-d_6$ ):  $\delta$  1.96–1.99 (t, 4H, Ben- $\text{CH}_2$ ):  $\delta$  3.35 (t, 4H, Ben- $\text{CH}_2\text{CH}_2$ ), 3.81 (d, 4H, NCH<sub>2</sub>), 6.53–7.57 (m, 8H, Ben-H), 7.88 (s, 2H, Phen-H), 8.09 (s, 2H, Phen-H), 8.59 (d, 2H, Phen-H).  $^{13}\text{C}$  NMR (125 MHz,  $\text{DMSO}-d_6$ ):  $\delta$  = 168.25; 155.05; 144.56; 129.20; 127.86; 125.92; 124.98; 124.82; 122.95; 40.12; 26.73; 23.75. FT-IR (KBr,  $\nu/\text{cm}^{-1}$ ): 1656 (amide), 1598, 1581, 1546, 1490, 1442, 1384, 1350, 1296, 1160, 1095, 896, 866. ESI-MS:  $m/z$  499.34 [ $\text{L} + \text{H}]^+$ , 521.34 [ $\text{L} + \text{Na}]^+$ .

**Solvent Extraction. Caution!** All radioactivity experiments were carried out in a glovebox under supervision. Trace amounts of  $^{241}\text{Am}$ (III) or Eu(III) were added to  $\text{NaNO}_3$  (1 M) solutions with different nitric acid concentrations (0.5–4 M) to prepare the aqueous phase. The organic phase was prepared by dissolving a certain concentration of QL-DAPhen in 3-nitrobenzotrifluoride. The mixture of the same amount (usually 1.0 mL) of aqueous solution and organic phase was shaken violently at  $25 \pm 1$  °C for 30 min in a constant-temperature oscillator to reach the extraction equilibrium. The  $\alpha$ -ray activity of  $^{241}\text{Am}$  (III) in aqueous solution before and after extraction

was determined by a low-background  $\alpha$ -scintillation detector. The distribution ratio ( $D_{\text{Am}}$ ) value was calculated by the ratio of the radioactive counts of the organic phase and the aqueous phase after extraction. The relative concentration of Eu(III) was determined by ICP-OES, and the distribution ratio ( $D_{\text{Eu}}$ ) values were calculated by the ratio of the concentration of the organic phase to the aqueous phase. The separation factor ( $SF_{\text{Am/Eu}}$ ) was calculated by the distribution ratio of  $^{241}\text{Am}$ (III) and Eu(III).

**ESI-MS Study.** The species changes of the complexes formed by QL-DAPhen and Eu(III) at different concentration ratios were studied by MS titration. For ESI-MS titration,  $\text{Eu}(\text{NO}_3)_3$  methanol solution (1 mM) was added into 1 mL of QL-DAPhen methanol (10 mM) to prepare a series of mother solutions, and they were oscillated in a thermostatic oscillator for 5 min to ensure complex equilibrium. The positive ion mode was used to analyze the titration solution on ESI-MS.

**UV-Vis Spectroscopy Study.** The coordination behavior of QL-DAPhen with Eu(III) in methanol/water (49/1) was determined by UV-vis spectrophotometry. In 0.02 mM QL-DAPhen aqueous solution (5 mL) containing 10 mM tetraethylammonium nitrate ( $\text{Et}_4\text{NNO}_3$ ), 10  $\mu\text{L}$  of 0.2 mM  $\text{Eu}(\text{NO}_3)_3$  in methanol (2% water) was added. The solution was oscillated vigorously in a thermostatic oscillator for 5 min at  $25 \pm 1$  °C to ensure complex equilibrium and then the absorbance of the solution was measured at 240–500 nm. The obtained spectral data were processed and fitted by the HypSpec program.

**$^1\text{H}$  NMR Spectroscopy Titration.** In the NMR titration experiments, we prepared the titration solution by dissolving the QL-DAPhen ligand and lanthanum nitrate into the solvent of  $\text{CD}_3\text{CN}/\text{CDCl}_3$ , respectively. For  $^1\text{H}$  NMR titration, 0.5 mL of the ligand solution was added to the NMR tube, and the spectra were recorded on a Bruker Avance III model 500 MHz instrument. Then, a certain volume of the lanthanum nitrate solvent was added to the NMR tube and ultrasonicated for 2 min after each addition to ensure

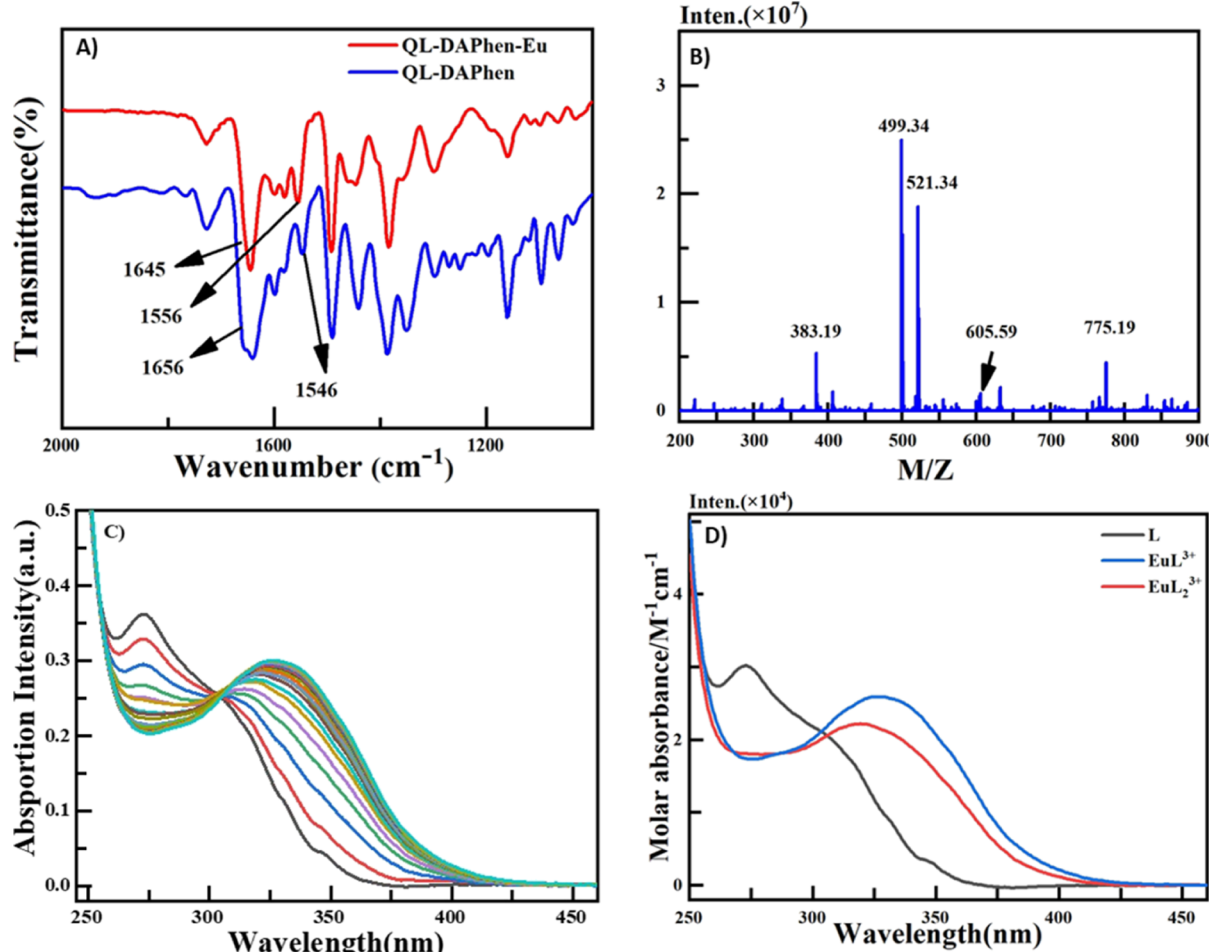


**Figure 3.** (A) FT-IR spectra of QL-DAPhen and its complex with Eu(III). (B) ESI-MS spectrum of the extracted organic phase in  $\text{CH}_3\text{OH}$ . (C) UV-vis titration spectra of QL-DAPhen with Eu(III) in  $\text{CH}_3\text{OH}/\text{H}_2\text{O}$  (49:1) ( $C_L = 2 \times 10^{-5} \text{ M}$ ,  $V_0 = 5 \text{ mL}$ ,  $C_{\text{Eu}} = 2.0 \times 10^{-4} \text{ M}$ ,  $T = 25^\circ\text{C}$ ,  $I = 0.01 \text{ M Et}_4\text{NNO}_3$ ). (D) Calculated molar absorptivity of QL-DAPhen and its complexes with Eu(III).

the complexation balance and then the corresponding  $^1\text{H}$  NMR spectra were recorded.

**Computational Details.** The complexation behaviors of Am(III) and Eu(III) with QL-DAPhen were optimized by using density functional theory (DFT),<sup>41</sup> and the BP86 pure functional,<sup>42</sup> with the Gaussian 16 program.<sup>43</sup> Relativistic effects were taken into consideration with the quasi-relativistic effective core potentials (RECPs)<sup>44,45</sup> for Am and Eu atoms, and the corresponding ECP28MWB-SEG<sup>44</sup> and ECP60MWB-SEG<sup>46,47</sup> valence basis sets were used, respectively. The 6-31G\* basis set was applied for C, N, O, and H. Optimizations of all the complexes were carried out at the BP86/6-31G\*/RECP level of theory in the gas phase without symmetry constraints. Harmonic vibrational frequencies were calculated to confirm the optimized structures to be the local minima on the potential energy surfaces. In order to take consideration of the solvent effect, the conductor-like screening model (COSMO)<sup>48,49</sup> was used to calculate solvation energies in the aqueous and 3-nitrotrifluorotoluene solution by using the BP86 functional with the larger 6-31G\*\* basis set based on the optimized structures in the gas phase.

## RESULTS AND DISCUSSION

**Solvent Extraction Studies.** For the solvent extraction, the QL-DAPhen ligand was dissolved in 3-nitrotrifluorotoluene solution as the organic phase, and a nitric acid solution containing Am(III) or Eu(III) ions and sodium nitrate salts was used as the aqueous phase. We evaluated the extraction

performance of the system by controlling the variables. First, considering that the acidity of the aqueous phase has a great influence on the extraction performance, we investigated the effect of nitric acid concentration (0.5–4 M) on the extraction of Am(III) and Eu(III). As shown in Figure 2A, with the concentration of nitric acid ranging from 0.5 to 3 M, the distribution ratio of Am(III) ( $D_{\text{Am}}$ ) and Eu(III) ( $D_{\text{Eu}}$ ) positively correlated to the acidity. When the nitric acid concentration reached 3 M, both  $D_{\text{Am}}$  and  $D_{\text{Eu}}$  reached the maximum value ( $D_{\text{Am}} = 17$  and  $D_{\text{Eu}} = 0.37$ ). Compared with the poor acid adaptability of the amide ligands containing only aliphatic chains,<sup>50</sup> the proper introduction of aromatic rings greatly improves the acid adaptability of the ligand. In addition, the ligand is highly selective for Am(III), and the separation factor ( $\text{SF}_{\text{Am/Eu}}$ ) exceeded 30 in a wide acidity range.

Considering the actual production, extraction kinetics is also one of the most important parameters to evaluate the extraction performance. Therefore, we explored the influence of the two-phase contact time on the extraction of Am(III) and Eu(III). As shown in Figure 2B, both  $D_{\text{Am}}$  and  $D_{\text{Eu}}$  changed with the increasing contact time of the two phases. The extraction of Am(III) and Eu(III) by the QL-DAPhen ligand reaches equilibrium at about 5 min, which is better than that at the equilibrium time of other phenanthroline-based ligands (these ligands reach extraction equilibrium within 20 min) for the extraction of trivalent ions.<sup>26,32,51,52</sup> This difference may be

due to the large quinoline group that enables the ligand to have higher preorganization capabilities. At equilibrium, the distribution ratio of Am(III) ( $D_{\text{Am}} = 17$ ) was 2 orders of magnitude larger than that of Eu(III) ( $D_{\text{Eu}} = 0.37$ ), which was roughly equivalent to the previously reported results obtained by the Et-Tol-DAPhen ligand in 3-nitrotrifluorotoluene.<sup>35</sup>

According to the reported works,<sup>53,54</sup>  $\text{NO}_3^-$  ions usually play an important role during extraction, so it is necessary to explore the effect of nitrate ions on the extraction process. By fixing 3 M HNO<sub>3</sub> and other conditions, NaNO<sub>3</sub> solution with different concentrations (0.5–1.5 M) was introduced to the extraction system. As shown in Figure 2C, the  $D_{\text{Am}}$  value increases with the increase of NO<sub>3</sub><sup>-</sup> ion concentration from 0.5 to 0.8 M, suggesting that nitrate ions may be involved during the extraction process. When the NaNO<sub>3</sub> concentration exceeded 1 M,  $D_{\text{M}}$  almost does not change, which is believed to be due to the competitive effect of Na<sup>+</sup> ions that offsets the promotion of NO<sub>3</sub><sup>-</sup> ions.<sup>53</sup>

It is well known that the  $D$  value is always dependent on the ligand concentration. Thus, we further evaluated the effect of ligand concentration from 2 mM to 50 mM on the extraction of Am(III) and Eu(III) by fixing 1 M HNO<sub>3</sub> and 0.1 mM Eu(III). As shown in Figure 2D, with the increasing ligand concentration, both  $D_{\text{Am}}$  and  $D_{\text{Eu}}$  were clearly enhanced. Then, slope analysis was used to determine the stoichiometry between the ligand and the metal ions. Based on the log–log curves of the ligand concentration versus the  $D$  values, the slopes of 1.37 and 1.46 for Am(III) and Eu(III) are obtained, respectively, which indicate that 1:1 and 1:2 complex species coexisted in the extracted organic phase for both Am(III) and Eu(III). This is slightly different from our previous study that reports that the Et-Tol-DAPhen ligand mainly generates 1:2 species (M–ligand) in the same extraction system.<sup>35</sup> The reason may be that the introduction of the quinoline group leads to an increase in the steric hindrance of the ligand, which hinders the 1:2 speciation.

**Complexation of Eu(III) with QL-DAPhen.** To understand the reason that the affinity of QL-DAPhen with Am(III) is stronger than Eu(III), the coordination behavior of the ligand with Lns(III) was studied in detail.

**FT-IR Spectroscopy Study.** Figure 3A shows the FT-IR spectra of the QL-DAPhen ligand and its Eu(III) complexes. The blue curve and the red curve correspond to the ligand and its complexes, respectively. The peaks at 1656 and 1546 cm<sup>-1</sup> are identified as the stretching vibration peaks of the C=O bond and the C=N bond of QL-DAPhen.<sup>32,54</sup> When the QL-DAPhen ligand was complexed with Eu(III), the peak for the C=O bond was red-shifted by 11 cm<sup>-1</sup>, which was caused by the carbonyl association. Inversely, the peak for the C=N bond was shifted by 10 cm<sup>-1</sup> in the direction of high wavenumber, which may be due to the change of  $\pi-\pi$  stacking.<sup>54</sup> The above infrared absorption changes indicate that QL-DAPhen complexes with Eu(III) through the C=O and C=N bonds in the ligand.

**ESI-MS Analysis.** In order to explore the species of the complex formed during the extraction, the coordination model of QL-DAPhen with Eu(III) was analyzed by ESI-MS in the positive mode. Figure 3B shows the mass spectrum of the extracted organic phase in methanol. The peaks at  $m/z$  383.19, 499.34, 605.59, and 775.19 are attributed to [2L + Eu]<sup>3+</sup>, [L + H]<sup>+</sup>, [2L + Eu + NO<sub>3</sub><sup>-</sup>]<sup>2+</sup>, and [L+2NO<sub>3</sub><sup>-</sup> + Eu]<sup>+</sup>, respectively. Considering that MS titration is an important means to explore the state change of complex species,<sup>55</sup> the titration analysis of

the solution with different Eu/L ratios in methanol solution was carried out. As shown in Figure 4 and Table S1, when the

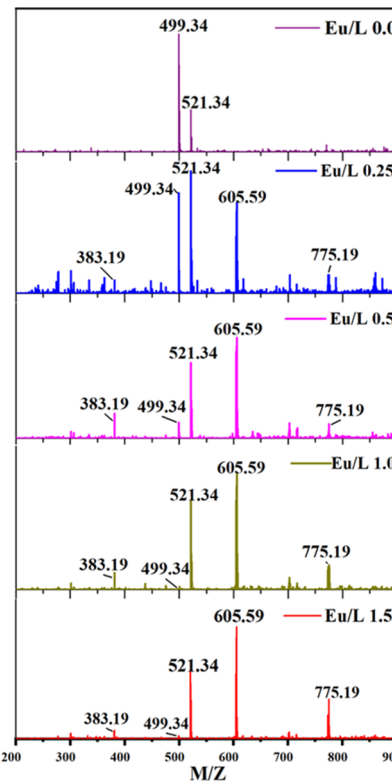


**Figure 4.** Mass spectrum titration of the complexes with different metal–ligand ratios (Eu/L) in CH<sub>3</sub>OH/H<sub>2</sub>O (49:1).

ratio of Eu/L  $\geq 0.25$ , two complexes of 1:1 and 1:2 are found with the corresponding  $m/z$  peaks. With the further increase of the ratio, these two complexes can still be observed. In order to confirm this result, we subsequently performed UV–vis titration.

**UV–Vis Spectroscopy Studies.** Figure 3C shows the UV–vis titration spectra of the ligand with Eu(III) in methanol/water (49/1) solution. With the increase of the concentration of Eu(III), the intensity of the absorption peak at 273 nm began to decrease, and a new absorption band appeared at  $\sim 318$  nm. When the ratio of Eu/L increased from 1 to 2, another new absorption band appeared at  $\sim 328$  nm, and the absorption intensity increased with the increase of Eu(III) concentration. With the further increase of Eu(III) concentration, the whole absorption band reached the titration endpoint. In addition, two isometric titration points appeared between 301 and 308 nm during the titration process, indicating that M/L = 1:1 and 1:2 species coexisted in the CH<sub>3</sub>OH/H<sub>2</sub>O solution.<sup>32,53,54</sup> The obtained spectra were fitted by HypSpec program,<sup>32</sup> and the stability constants  $\log \beta_{[\text{EuL}]}$  and  $\log \beta_{[\text{EuL}2]}$  were calculated as 5.2 and 9.4, respectively. This result proves that the 1:1 species formed by Eu(III) and QL-DAPhen are more stable than the 1:2 species. The absorption spectra of the ligand and the two complexes are given in Figure 3D, from which the three species can be easily distinguished from each other. In addition, the absorption spectra of La/L were also obtained (see in Figure S5). With the addition of La(III), new absorption peaks appeared at 319 nm and 332 nm successively, and an isometric titration point appeared at 305 nm. Spectroscopic analysis

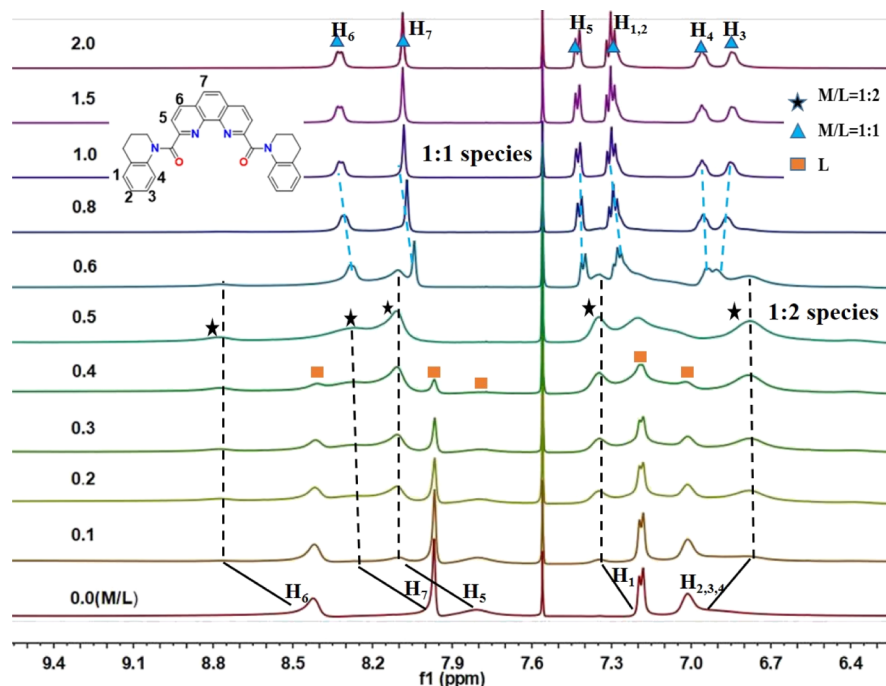


**Figure 5.** Stacked  $^1\text{H}$  NMR spectra (6.20–9.60 ppm) of QL-DAPhen (20.0 mM) titrated with  $\text{La}(\text{NO}_3)_3$  in the mixture of  $\text{CD}_3\text{CN}/\text{CDCl}_3$  (v/v, 7/3) at 295 K. M/L denotes the molar ratio of  $\text{La}(\text{III})$  with QL-DAPhen in the tested samples.

showed that  $\text{LaL}$  and  $\text{LaL}_2$  coexist in the solution. This change in trend is consistent with the Eu/L titration, which shows that La/L and Eu/L have similar species distributions.

**NMR Titration Spectroscopy Analysis.** NMR spectroscopy with high sensitivity is often used to determine the stoichiometric number of ligand molecules and diamagnetic metal ions.<sup>36,37,56–58</sup> Considering that Eu(III) is paramagnetic, we use diamagnetic La(III) as a substitute for the titration. Figure 5 shows the  $^1\text{H}$  NMR titration spectra of the ligand with different concentrations of  $\text{La}(\text{NO}_3)_3$ , ranging from 6.20 to 9.60 ppm. In the absence of  $\text{La}(\text{NO}_3)_3$ , the proton peaks at 8.41, 7.97, and 7.82 ppm in the spectra are from 1,10-phenanthroline. According to the analysis of the  $^1\text{H}$  NMR spectrum of QL-DAPhen in Figure S3 and the  $^1\text{H}-^1\text{H}$ -COSY spectrum of the ligand in Figure S4, these peaks are attributed to  $\text{H}_6$ ,  $\text{H}_7$ , and  $\text{H}_5$ , respectively. The shifts between 6.50 and 7.20 ppm are attributed to the proton signals on the benzene ring. With the addition of La(III), five new broadening peaks (marked with black stars) were generated, which reached the maximum when the M/L ratio was in the range of 0.5–0.6, while the residual ligand peaks almost disappeared. With the further addition of La(III), these broadening peaks gradually weakened, and another new set of NMR signals appeared (marked with blue triangles) at  $\text{M/L} \geq 0.6$ , which then tended to be stable at  $\text{M/L} \geq 1.5$ . The above trends can be successfully matched with the formation trend of  $\text{LaL}_2$  and  $\text{LaL}$  during the titration (see Figure S5). Specially, when  $\text{M/L} < 0.6$ , the broadened peaks represent the protons of QL-DAPhen as two forms: free ligand and binding to La(III) in the complex  $\text{LaL}_2$ . The peak broadening is caused by ligand exchange; when  $\text{M/L} \geq 0.6$ , the complex  $\text{LaL}$  formed and tended to be predominant at  $\text{M/L} > 1.5$ . According to the similar chemical properties of trivalent lanthanides and actinides and other spectroscopic results, Am(III) and Eu(III) will also exist in the organic phase as similar species when they are complexed with QL-DAPhen.

**DFT Calculations.** The theoretical method adopted in this study has been widely used to study the complexing behavior of Am(III) and Eu(III) with ligands.<sup>59,60</sup> To illustrate the geometric and electronic structures of Am(III) and Eu(III) complexes with QL-DAPhen (L), we optimized the structures of 1:1 species  $\text{AmL}(\text{NO}_3)_3/\text{EuL}(\text{NO}_3)_3$  and 1:2 species  $[\text{Am}(\text{L})_2(\text{NO}_3)]^{2+}/[\text{Eu}(\text{L})_2(\text{NO}_3)]^{2+}$  according to the experimental results, as shown in Figure 6. The M–N and M–O bond lengths in  $\text{ML}(\text{NO}_3)_3$  and  $[\text{ML}_2(\text{NO}_3)]^+$  (M = Am, Eu) complexes at the BP86/6-31G\*/RECP level of theory are

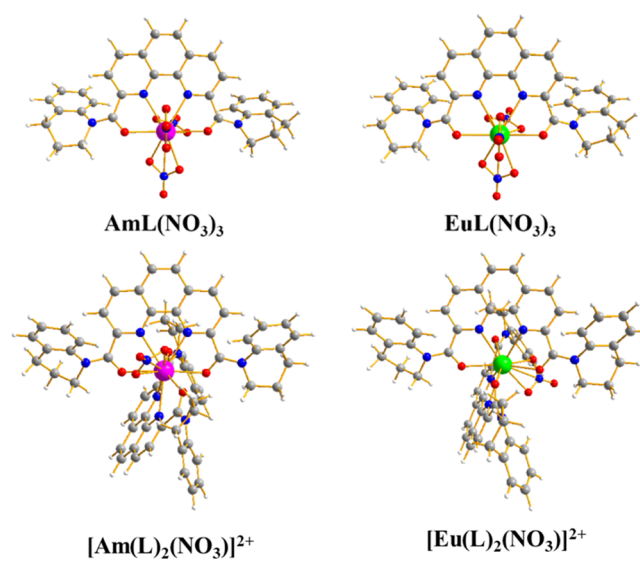


**Figure 6.** Optimized structures of the  $\text{ML}(\text{NO}_3)_3$  and  $[\text{M}(\text{L})_2(\text{NO}_3)]^{2+}$  ( $\text{M} = \text{Am}(\text{III})$  and  $\text{Eu}(\text{III})$ ) complexes at the BP86/6-31G\*/RECP level of theory in the gas phase. H, C, N, O, Am, and Eu atoms are represented by white, gray, blue, red, pink, and green spheres, respectively.

**Table 1.** Average M–O and M–N Bond Lengths (Å), WBIs of M–O and M–N Bonds, and Mulliken Charges on the O, N, and M Atoms in the  $\text{ML}(\text{NO}_3)_3$  and  $[\text{ML}_2(\text{NO}_3)]^{2+}$  Complexes

complexes	bond length		WBIs		Mulliken charge		
	M–O	M–N	M–O	M–N	$Q_{\text{O}}$	$Q_{\text{N}}$	$Q_{\text{M}}$
$\text{EuL}(\text{NO}_3)_3$	2.568	2.701	0.196	0.166	−0.437	−0.478	1.268
$\text{AmL}(\text{NO}_3)_3$	2.525	2.653	0.249	0.219	−0.434	−0.488	1.174
$[\text{EuL}_2(\text{NO}_3)]^{2+}$	2.540	2.676	0.228	0.188	−0.461	−0.502	1.237
$[\text{AmL}_2(\text{NO}_3)]^{2+}$	2.541	2.636	0.258	0.232	−0.453	−0.501	1.152

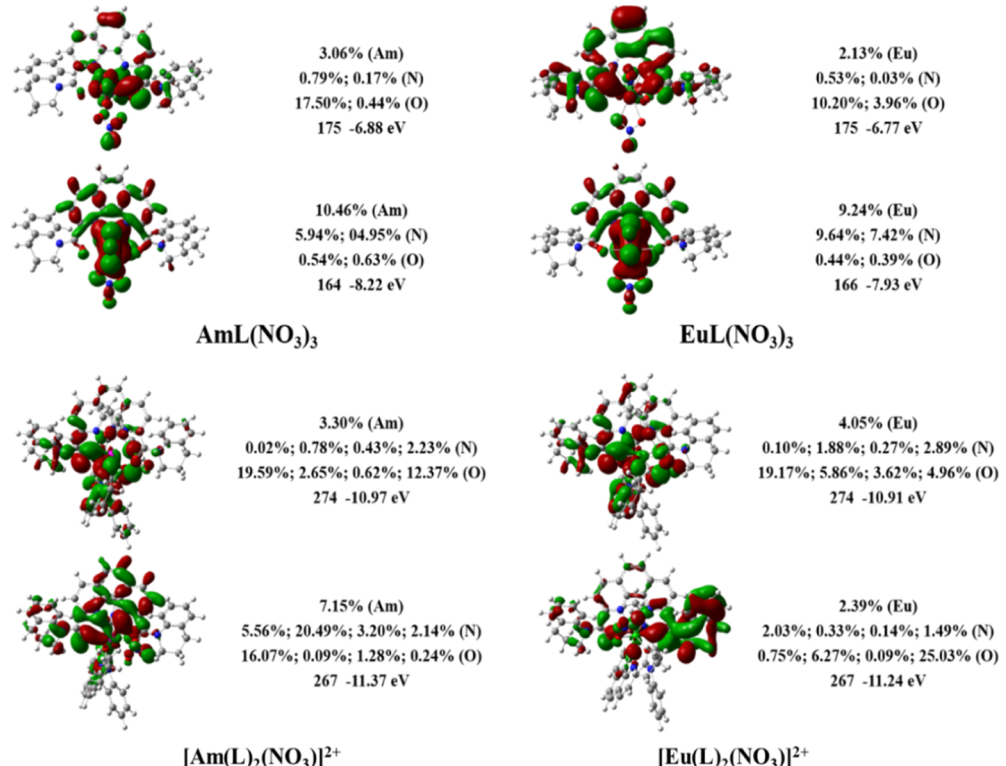


**Figure 7.** Composition and energy level (eV) of the  $\alpha$ -spin valence MOs of the  $\text{ML}(\text{NO}_3)_3$  and  $[\text{M(L)}_2(\text{NO}_3)]^{2+}$  complexes obtained at the BP86/6-31G\*/RECP level of theory in the gas phase. The isosurface value is set as 0.02 au.

**Table 2.** Changes in Gibbs Free Energy ( $\Delta G$ , kcal/mol) for the Reactions of QL-DAPhen and  $[\text{M}(\text{NO}_3)(\text{H}_2\text{O})_8]^{2+}$  and  $\text{NO}_3^-$  in Gas and Aqueous and 3-Nitrotrifluorotoluene Solutions at the BP86/6-311G\*\*/RECP Level of Theory<sup>a</sup>

complexes	$[\text{M}(\text{NO}_3)(\text{H}_2\text{O})_8]^{2+} + \text{L} + 2\text{NO}_3^- = \text{ML}(\text{NO}_3)_3 + 8\text{H}_2\text{O}$					
	$\Delta G_{\text{gas}}$	$\Delta\Delta G_{\text{gas}}$	$\Delta G_{\text{aq}}$	$\Delta\Delta G_{\text{aq}}$	$\Delta G_{3\text{-nit}}$	$\Delta\Delta G_{3\text{-nit}}$
$\text{ML}(\text{NO}_3)_3$	−297.3/−302.49	−5.19	−51.11/−55.66	−4.54	−50.48/−54.97	−4.49
			$[\text{M}(\text{NO}_3)(\text{H}_2\text{O})_8]^{2+} + 2\text{L} = [\text{ML}_2(\text{NO}_3)]^{2+} + 8\text{H}_2\text{O}$			
complexes	$\Delta G_{\text{gas}}$	$\Delta\Delta G_{\text{gas}}$	$\Delta G_{\text{aq}}$	$\Delta\Delta G_{\text{aq}}$	$\Delta G_{3\text{-nit}}$	$\Delta\Delta G_{3\text{-nit}}$
$[\text{ML}_2(\text{NO}_3)]^{2+}$	−100.49/−104.49	−4.00	−46.29/−48.21	−1.92	−44.13/−46.07	−1.93

<sup>a</sup>The results of Eu(III) and Am(III) complexes, respectively.

presented in Table 1. All the Am–N and Am–O bonds are somewhat shorter than the corresponding Eu–N and Eu–O bonds, respectively, which shows that QL-DAPhen has a stronger complexing ability to Am(III). For example, the Am–N bond (2.653 Å) is shorter than the Eu–N bond (2.701 Å) for the  $\text{ML}(\text{NO}_3)_3$  complexes.

To explore the bonding nature of the metal–ligand (M–L) bonds, the natural bonding orbital analyses of all the complexes were performed at the BP86/6-31G\*/RECP level of theory. The Wiberg bond index (WBI) is regarded as an effective factor to measure the degree of covalency.<sup>32,61</sup> As listed in Table 1, all the values of the WBIs are within the range of

0.166–0.258, indicating that the interactions between the ligands and the metal ions show weak covalency. Furthermore, the values of WBIs for the Am–N and Am–O bonds are larger than those for their Eu counterparts, respectively, denoting the more covalency present in Am–L bonds. Besides, the Mulliken charges on the metal and the N and O atoms are also listed in Table 1. Obviously, the Mulliken charges located on the Am atoms are smaller than those of Eu atoms in the same type of complexes, showing a larger charge transfer from the ligands to Am ions. This result indicates that QL-DAPhen has a stronger coordinating ability to Am(III) compared to Eu(III).

The  $\alpha$ -spin valence molecular orbitals (MOs) and their composition in the  $\text{ML}(\text{NO}_3)_3$  and  $[\text{ML}_2(\text{NO}_3)]^{2+}$  complexes are illustrated in Figure 7. It is clearly seen that the bonds between metal atoms and N/O atoms have an obvious  $\sigma$  character. The energy levels of MOs in the Am complexes are somewhat lower than those in the Eu counterparts, while the Am and Eu complexes have similar bonding interactions. This result indicates that the ligand has a better complexing ability with Am(III) than with Eu(III).

The changes in Gibbs free energy ( $\Delta G$ ) for the reactions in the gas and aqueous (aq.) and 3-nitrotrifluorotoluene (3-nit.) solutions were calculated at the BP86/6-311G\*\*/RECP level of theory, as given in Table 2. The  $\Delta G$  value for the reaction with Am(III) complexes is more negative than that with Eu(III) complexes, indicating that QL-DAPhen has a stronger complexing ability toward Am(III) than toward Eu(III). The  $\Delta G$  values for the reactions of  $\text{ML}(\text{NO}_3)_3$  complexes are more negative than those of  $[\text{M(L)}_2(\text{NO}_3)]^{2+}$  ones, revealing that the 1:1 metal/ligand complex  $\text{ML}(\text{NO}_3)_3$  is the predominant species in the extracted organic phase. According to the formula  $\Delta\Delta G = -RT \ln SF_{\text{Am/Eu}}$  ( $T = 298$  K) and the experimental separation factors ( $SF_{\text{Am/Eu}}$ ) of 45 (3 M  $\text{HNO}_3$ ), we can obtain the value of  $\Delta\Delta G$  as  $-2.24$  kcal/mol. Therefore, the calculated  $\Delta G$  value in the 3-nitrotrifluorotoluene solution is in agreement with the experimental result.

## CONCLUSIONS

In this work, a novel tetradentate amide ligand, 2,9-diacyl-bis((3,4-dihydroquinoline-1(2H)-yl)-1),10-phenanthroline (QL-DAPhen), has been synthesized, which can be used to separate trivalent actinides from lanthanides with high efficiency and selectivity in a high acid medium. The slope analysis results indicate that 1:1 and 1:2 extraction species are formed during the extraction process. The NMR titration, UV-vis spectrophotometric titration, and ESI-MS studies reveal that the 1:1 and 1:2 complex species coexist in the organic phase. The thermodynamic calculations confirm that the formation of the 1:1 complex has more thermodynamic advantages than the 1:2 complex under the extraction conditions. In addition, the DFT calculation results show that the Am-L bonds in the complexes have more covalent properties than the Eu-L bonds. This study clearly illustrates that the tailoring ligand framework will change the species distribution during the extraction, which provides a certain reference value for the design of the actinide extractant.

## ASSOCIATED CONTENT

### Supporting Information

The Supporting Information is available free of charge at <https://pubs.acs.org/doi/10.1021/acs.inorgchem.1c02916>.

Equations; NMR spectra of QL-DAPhen; UV-vis titration spectral analysis; MS analysis; and Cartesian coordinates of optimized structures (PDF)

## AUTHOR INFORMATION

### Corresponding Authors

Li-yong Yuan – Laboratory of Nuclear Energy Chemistry, Institute of High Energy Physics, Chinese Academy of Sciences, Beijing 100049, P.R. China; [orcid.org/0000-0003-4261-8717](https://orcid.org/0000-0003-4261-8717); Email: [yuanly@ihep.ac.cn](mailto:yuanly@ihep.ac.cn)

Wei-qun Shi – Laboratory of Nuclear Energy Chemistry, Institute of High Energy Physics, Chinese Academy of

Sciences, Beijing 100049, P.R. China; [orcid.org/0000-0001-9929-9732](https://orcid.org/0000-0001-9929-9732); Email: [shiwq@ihep.ac.cn](mailto:shiwq@ihep.ac.cn)

### Authors

Shuai Wang – Radiochemistry Laboratory, School of Nuclear Science and Technology, Lanzhou University, Lanzhou 730000, P.R. China; Laboratory of Nuclear Energy Chemistry, Institute of High Energy Physics, Chinese Academy of Sciences, Beijing 100049, P.R. China

Cui Wang – Laboratory of Nuclear Energy Chemistry, Institute of High Energy Physics, Chinese Academy of Sciences, Beijing 100049, P.R. China

Xiao-fan Yang – Laboratory of Nuclear Energy Chemistry, Institute of High Energy Physics, Chinese Academy of Sciences, Beijing 100049, P.R. China; Department of Radiochemistry, China Institute of Atomic Energy, Beijing 102413, P.R. China; [orcid.org/0000-0002-4916-7050](https://orcid.org/0000-0002-4916-7050)

Ji-pan Yu – Laboratory of Nuclear Energy Chemistry, Institute of High Energy Physics, Chinese Academy of Sciences, Beijing 100049, P.R. China

Wu-qing Tao – Department of Radiochemistry, China Institute of Atomic Energy, Beijing 102413, P.R. China

Su-liang Yang – Department of Radiochemistry, China Institute of Atomic Energy, Beijing 102413, P.R. China

Peng Ren – Laboratory of Nuclear Energy Chemistry, Institute of High Energy Physics, Chinese Academy of Sciences, Beijing 100049, P.R. China

Zhi-fang Chai – Radiochemistry Laboratory, School of Nuclear Science and Technology, Lanzhou University, Lanzhou 730000, P.R. China; Laboratory of Nuclear Energy Chemistry, Institute of High Energy Physics, Chinese Academy of Sciences, Beijing 100049, P.R. China; Engineering Laboratory of Advanced Energy Materials, Ningbo Institute of Materials Technology and Engineering, Chinese Academy of Sciences, Ningbo 315201, P.R. China

Complete contact information is available at:

<https://pubs.acs.org/10.1021/acs.inorgchem.1c02916>

### Author Contributions

<sup>1</sup>S.W. and C.W. contributed equally and should be considered co-first authors.

### Notes

The authors declare no competing financial interest.

## ACKNOWLEDGMENTS

This work was supported by the National Natural Science Foundation of China (nos. 22076188, U1967216, U2032106, and 11875058) and the National Science Fund for Distinguished Young Scholars (no. 21925603).

## REFERENCES

- (1) González-Romero, E. M. Impact of partitioning and transmutation on the high level waste management. *Nucl. Eng. Des.* **2011**, *241*, 3436–3444.
- (2) Salvatores, M. Nuclear fuel cycle strategies including Partitioning and Transmutation. *Nucl. Eng. Des.* **2005**, *235*, 805–816.
- (3) Salvatores, M.; Palmiotti, G. Radioactive waste partitioning and transmutation within advanced fuel cycles: Achievements and challenges. *Prog. Part. Nucl. Phys.* **2011**, *66*, 144–166.
- (4) Herbst, R. S.; Baron, P.; Nilsson, M., Standard and advanced separation: PUREX processes for nuclear fuel reprocessing. *Advanced Separation Techniques for Nuclear Fuel Reprocessing and Radioactive Waste Treatment*; Woodhead Publishing, 2011; pp 141–175.

- (5) Magill, J.; Berthou, V.; Haas, D.; Galy, J.; Schenkel, R.; Wiese, H.-W.; Heusener, G.; Tommasi, J.; Youinou, G. Impact limits of partitioning and transmutation scenarios on the radiotoxicity of actinides in radioactive waste. *Nucl. Energy* **2003**, *42*, 263–277.
- (6) Baisden, P. A.; Choppin, G. R. Nuclear Waste Management and The Nuclear Fuel Cycle. Nuclear Waste Management and The Nuclear Fuel Cycle. In *Radiochemistry and Nuclear Chemistry*; Nagyl, S., Ed.; EOLSS Publishers: Oxford, U.K., 2007; pp 1–63.
- (7) Wang, C.; Wu, Q.-Y.; Kong, X.-H.; Wang, C.-Z.; Lan, J.-H.; Nie, C.-M.; Chai, Z.-F.; Shi, W.-Q. Theoretical Insights into the Selective Extraction of Americium(III) over Europium(III) with Dithioamide-Based Ligands. *Inorg. Chem.* **2019**, *58*, 10047–10056.
- (8) Dam, H. H.; Reinhoudt, D. N.; Verboom, W. Multicoordinate ligands for actinide/lanthanide separations. *Chem. Soc. Rev.* **2007**, *36*, 367–377.
- (9) Zhu, Y. The Separation of Americium from Light Lanthanides by Cyanex 301 Extraction. *Radiochim. Acta* **1995**, *68*, 95–98.
- (10) Modolo, G.; Odoj, R. Synergistic selective extraction of actinides(III) over lanthanides from nitric acid using new aromatic diorganyldithiophosphinic acids and neutral organophosphorus compounds. *Solvent Extr. Ion Exch.* **1999**, *17*, 33–53.
- (11) Lan, J.-H.; Shi, W.-Q.; Yuan, L.-Y.; Feng, Y.-X.; Zhao, Y.-L.; Chai, Z.-F. Thermodynamic Study on the Complexation of Am(III) and Eu(III) with Tetridentate Nitrogen Ligands: A Probe of Complex Species and Reactions in Aqueous Solution. *J. Phys. Chem. A* **2012**, *116*, 504–511.
- (12) Hudson, M. J.; Harwood, L. M.; Laventine, D. M.; Lewis, F. W. Use of Soft Heterocyclic N-Donor Ligands To Separate Actinides and Lanthanides. *Inorg. Chem.* **2013**, *52*, 3414–3428.
- (13) Adam, C.; Beele, B. B.; Geist, A.; Müllrich, U.; Kaden, P.; Panak, P. J. NMR and TRLFS studies of Ln(III) and An(III) CS-BPP complexes. *Chem. Sci.* **2015**, *6*, 1548–1561.
- (14) Sole, K. C.; Brent Hiskey, J.; Ferguson, T. L. An Assessment of the Long-term Stabilities of Cyanex302 and Cyanex301 in Sulfuric and Nitric Acids. *Solvent Extr. Ion Exch.* **1993**, *11*, 783–796.
- (15) Modolo, G.; Odoj, R. The separation of trivalent actinides from lanthanides by dithiophosphinic acids from HNO<sub>3</sub> acid medium. *J. Alloys Compd.* **1998**, *271*–273, 248–251.
- (16) Marc, P.; Custelcean, R.; Groenewold, G. S.; Klaehn, J. R.; Peterman, D. R.; Delmau, L. H. Degradation of CYANEX 301 in Contact with Nitric Acid Media. *Ind. Eng. Chem. Res.* **2012**, *51*, 13238–13244.
- (17) Nash, K. L. The Chemistry of TALSPEAK: A Review of the Science. *Solvent Extr. Ion Exch.* **2015**, *33*, 1–55.
- (18) Chandrasekar, A.; Ghanty, T. K. Uncovering Heavy Actinide Covalency: Implications for Minor Actinide Partitioning. *Inorg. Chem.* **2019**, *58*, 3744–3753.
- (19) Wang, Z.; Pu, N.; Tian, Y.; Xu, C.; Wang, F.; Liu, Y.; Zhang, L.; Chen, J.; Ding, S. Highly Selective Separation of Actinides from Lanthanides by Dithiophosphinic Acids: An in-Depth Investigation on Extraction, Complexation, and DFT Calculations. *Inorg. Chem.* **2019**, *58*, 5457–5467.
- (20) Modolo, G.; Odoj, R. Influence of the purity and irradiation stability of cyanex301 on the separation of trivalent actinides from lanthanides by solvent extraction. *J. Radioanal. Nucl. Chem.* **1998**, *228*, 83–88.
- (21) Bhattacharyya, A.; Mohapatra, P. K.; Manchanda, V. K. Solvent extraction and extraction chromatographic separation of Am<sup>3+</sup> and Eu<sup>3+</sup> from nitrate medium using Cyanex (R) 301. *Solvent Extr. Ion Exch.* **2007**, *25*, 27–39.
- (22) Jensen, M. P.; Bond, A. H. Influence of aggregation on the extraction of trivalent lanthanide and actinide cations by purified Cyanex 272, Cyanex 301, and Cyanex 302. *Radiochim. Acta* **2002**, *90*, 205–209.
- (23) Cao, X.; Heidelberg, D.; Ciupka, J.; Dolg, M. First-Principles Study of the Separation of AmIII/CmIII from EuIII with Cyanex301. *Inorg. Chem.* **2010**, *49*, 10307–10315.
- (24) Kolarik, Z.; Müllrich, U.; Gassner, F. SELECTIVE EXTRACTION OF Am(III) OVER Eu(III) BY 2,6-DITRIAZOLYL- AND 2,6-DITRIAZINYL PYRIDINES1. *Solvent Extr. Ion Exch.* **1999**, *17*, 23–32.
- (25) Foreman, M. R. S.; Hudson, M. J.; Drew, M. G. B.; Hill, C.; Madic, C. Complexes formed between the quadridentate, heterocyclic molecules 6,6'-bis-(5,6-dialkyl-1,2,4-triazin-3-yl)-2,2'-bipyridine (BTBP) and lanthanides(iii): implications for the partitioning of actinides(iii) and lanthanides(iii). *Dalton Trans.* **2006**, 1645–1653.
- (26) Lewis, F. W.; Harwood, L. M.; Hudson, M. J.; Drew, M. G. B.; Desreux, J. F.; Vidick, G.; Bouslimani, N.; Modolo, G.; Wilden, A.; Sympula, M.; Vu, T.-H.; Simonin, J.-P. Highly Efficient Separation of Actinides from Lanthanides by a Phenanthroline-Derived Bis-triazine Ligand. *J. Am. Chem. Soc.* **2011**, *133*, 13093–13102.
- (27) Lewis, F. W.; Harwood, L. M.; Hudson, M. J.; Drew, M. G. B.; Hubscher-Bruder, V.; Videva, V.; Arnaud-Neu, F.; Stamberg, K.; Vyas, S. BTBPs versus BTPhens: Some Reasons for Their Differences in Properties Concerning the Partitioning of Minor Actinides and the Advantages of BTPhens. *Inorg. Chem.* **2013**, *52*, 4993–5005.
- (28) Liu, Y.; Yang, X.; Ding, S.; Wang, Z.; Zhang, L.; Song, L.; Chen, Z.; Wang, X. Highly Efficient Trivalent Americium/Europium Separation by Phenanthroline-Derived Bis(pyrazole) Ligands. *Inorg. Chem.* **2018**, *57*, 5782–5790.
- (29) Modolo, G.; Wilden, A.; Daniels, H.; Geist, A.; Magnusson, D.; Malmbeck, R. Development and demonstration of a new SANEX Partitioning Process for selective actinide(III)/lanthanide(III) separation using a mixture of CyMe4BTBP and TODGA. *Radiochim. Acta* **2013**, *101*, 155–162.
- (30) Geist, A.; Hill, C.; Modolo, G.; Foreman, M. R. S. J.; Weigl, M.; Gompper, K.; Hudson, M. J. 6,6'-Bis(5,5,8,8-tetramethyl-5,6,7,8-tetrahydro-benzo[1,2,4]triazin-3-yl) [2,2']bipyridine, an Effective Extracting Agent for the Separation of Americium(III) and Curium(III) from the Lanthanides. *Solvent Extr. Ion Exch.* **2006**, *24*, 463–483.
- (31) Galletta, M.; Scaravaggi, S.; Macerata, E.; Famulari, A.; Mele, A.; Panzeri, W.; Sansone, F.; Casnati, A.; Mariani, M. 2,9-Dicarbonyl-1,10-phenanthroline derivatives with an unprecedented Am(III)/Eu(III) selectivity under highly acidic conditions. *Dalton Trans.* **2013**, *42*, 16930–16938.
- (32) Xiao, C.-L.; Wang, C.-Z.; Yuan, L.-Y.; Li, B.; He, H.; Wang, S.; Zhao, Y.-L.; Chai, Z.-F.; Shi, W.-Q. Excellent Selectivity for Actinides with a Tetridentate 2,9-Diamide-1,10-Phenanthroline Ligand in Highly Acidic Solution: A Hard-Soft Donor Combined Strategy. *Inorg. Chem.* **2014**, *53*, 1712–1720.
- (33) Lavrov, H. V.; Ustynyuk, N. A.; Matveev, P. I.; Gloriozov, I. P.; Zhokhov, S. S.; Alyapshev, M. Y.; Tkachenko, L. I.; Voronaev, I. G.; Babain, V. A.; Kalmykov, S. N.; Ustynyuk, Y. A. A novel highly selective ligand for separation of actinides and lanthanides in the nuclear fuel cycle. Experimental verification of the theoretical prediction. *Dalton Trans.* **2017**, *46*, 10926–10934.
- (34) Karslyan, Y.; Sloop, F. V.; Delmau, L. H.; Moyer, B. A.; Popovs, I.; Paulenova, A.; Jansone-Popova, S. Sequestration of trivalent americium and lanthanide nitrates with bis-lactam-1,10-phenanthroline ligand in a hydrocarbon solvent. *RSC Adv.* **2019**, *9*, 26537–26541.
- (35) Zhang, X.; Wu, Q.; Lan, J.; Yuan, L.; Xu, C.; Chai, Z.; Shi, W. Highly selective extraction of Pu (IV) and Am (III) by N,N'-diethyl-N,N'-ditolyl-2,9-diamide-1,10-phenanthroline ligand: An experimental and theoretical study. *Sep. Purif. Technol.* **2019**, *223*, 274–281.
- (36) Xu, L.; Pu, N.; Li, Y.; Wei, P.; Sun, T.; Xiao, C.; Chen, J.; Xu, C. Selective Separation and Complexation of Trivalent Actinide and Lanthanide by a Tetridentate Soft-Hard Donor Ligand: Solvent Extraction, Spectroscopy, and DFT Calculations. *Inorg. Chem.* **2019**, *58*, 4420–4430.
- (37) Xu, L.; Pu, N.; Ye, G.; Xu, C.; Chen, J.; Zhang, X.; Lei, L.; Xiao, C. Unraveling the complexation mechanism of actinide(III) and lanthanide(III) with a new tetridentate phenanthroline-derived phosphonate ligand. *Inorg. Chem. Front.* **2020**, *7*, 1726–1740.
- (38) Babain, V. A.; Alyapshev, M. Y.; Kiseleva, R. N. Metal extraction by N,N'-dialkyl-N,N'-diaryl-dipicolinamides from nitric acid solutions. *Radiochim. Acta* **2007**, *95*, 217–223.

- (39) Chandler, C. J.; Deady, L. W.; Reiss, J. A. Synthesis of some 2,9-disubstituted-1,10-phenanthrolines. *J. Heterocycl. Chem.* **1981**, *18*, 599–601.
- (40) Chandler, C. J.; Deady, L. W.; Reiss, J. A.; Tzimos, V. The synthesis of macrocyclic polyether-diesters incorporating 1,10-phenanthrolino and 1,8-naphthyridino subunits. *J. Heterocycl. Chem.* **1982**, *19*, 1017–1019.
- (41) Cao, X.; Li, Q.; Moritz, A.; Xie, Z.; Dolg, M.; Chen, X.; Fang, W. Density functional theory studies of actinide(III) motexafins ( $\text{An}-\text{Motex}^{2+}$ ,  $\text{An} = \text{Ac}, \text{Cm}, \text{Lr}$ ). Structure, stability, and comparison with lanthanide(III) motexafins. *Inorg. Chem.* **2006**, *45*, 3444–3451.
- (42) Frisch, M. J.; Trucks, G. W.; Schlegel, H. B.; Scuseria, G. E.; Robb, M. A.; Cheeseman, J. R.; Scalmani, G.; Barone, V.; Petersson, G. A.; Nakatsuji, H.; Li, X.; Caricato, M.; Marenich, A. V.; Bloino, J.; Janesko, B. G.; Gomperts, R.; Mennucci, B.; Hratchian, H. P.; Ortiz, J. V.; Izmaylov, A. F.; Sonnenberg, J. L.; Williams-Young, D.; Ding, F.; Lipparini, F.; Egidi, F.; Goings, J.; Peng, B.; Petrone, A.; Henderson, T.; Ranasinghe, D.; Zakrzewski, V. G.; Gao, J.; Rega, N.; Zheng, G.; Liang, W.; Hada, M.; Ehara, M.; Toyota, K.; Fukuda, R.; Hasegawa, J.; Ishida, M.; Nakajima, T.; Honda, Y.; Kitao, O.; Nakai, H.; Vreven, T.; Throssell, K.; Montgomery, J. A., Jr.; Peralta, J. E.; Ogliaro, F.; Bearpark, M. J.; Heyd, J. J.; Brothers, E. N.; Kudin, K. N.; Staroverov, V. N.; Keith, T. A.; Kobayashi, R.; Normand, J.; Raghavachari, K.; Rendell, A. P.; Burant, J. C.; Iyengar, S. S.; Tomasi, J.; Cossi, M.; Millam, J. M.; Klene, M.; Adamo, C.; Cammi, R.; Ochterski, J. W.; Martin, R. L.; Morokuma, K.; Farkas, O.; Foresman, J. B.; Fox, D. J. *Gaussian 16*; Gaussian, Inc., 2016.
- (43) Dolg, M.; Stoll, H.; Preuss, H. Energy-adjusted ab initio pseudopotentials for the rare earth elements. *J. Chem. Phys.* **1989**, *90*, 1730–1734.
- (44) Küchle, W.; Dolg, M.; Stoll, H.; Preuss, H. Energy-adjusted pseudopotentials for the actinides. Parameter sets and test calculations for thorium and thorium monoxide. *J. Chem. Phys.* **1994**, *100*, 7535–7542.
- (45) Cao, X.; Dolg, M. Segmented contraction scheme for small-core lanthanide pseudopotential basis sets. *J. Mol. Struct.: THEOCHEM* **2002**, *581*, 139–147.
- (46) Cao, X.; Dolg, M.; Stoll, H. Valence basis sets for relativistic energy-consistent small-core actinide pseudopotentials. *J. Chem. Phys.* **2003**, *118*, 487–496.
- (47) Cao, X.; Dolg, M. Segmented contraction scheme for small-core actinide pseudopotential basis sets. *J. Mol. Struct.: THEOCHEM* **2004**, *673*, 203–209.
- (48) Klamt, A.; Schüürmann, G. COSMO: a new approach to dielectric screening in solvents with explicit expressions for the screening energy and its gradient. *J. Chem. Soc., Perkin Trans. 1* **1993**, *5*, 799–805.
- (49) Klamt, A.; Jonas, V.; Bürger, T.; Lohrenz, J. C. W. Refinement and parametrization of COSMO-RS. *J. Phys. Chem. A* **1998**, *102*, 5074–5085.
- (50) Manna, D.; Mula, S.; Bhattacharyya, A.; Chattopadhyay, S.; Ghanty, T. K. Actinide selectivity of 1, 10-phenanthroline-2, 9-dicarboxamide and its derivatives: a theoretical prediction followed by experimental validation. *Dalton Trans.* **2015**, *44*, 1332–1340.
- (51) Zaytsev, A. V.; Bulmer, R.; Kozhevnikov, V. N.; Sims, M.; Modolo, G.; Wilden, A.; Waddell, P. G.; Geist, A.; Panak, P. J.; Wessling, P.; Lewis, F. W. Exploring the Subtle Effect of Aliphatic Ring Size on Minor Actinide-Extraction Properties and Metal Ion Speciation in Bis-1,2,4-Triazine Ligands. *Chem.—Eur. J.* **2020**, *26*, 428–437.
- (52) Liu, Y.; Yang, X.; Ding, S.; Wang, Z.; Zhang, L.; Song, L.; Chen, Z.; Wang, X. Highly Efficient Trivalent Americium/Europium Separation by Phenanthroline-Derived Bis(pyrazole) Ligands. *Inorg. Chem.* **2018**, *57*, 5782–5790.
- (53) Li, Y.; Dong, X.; Yuan, J.; Pu, N.; Wei, P.; Sun, T.; Shi, W.; Chen, J.; Wang, J.; Xu, C. Performance and Mechanism for the Selective Separation of Trivalent Americium from Lanthanides by a Tetradentate Phenanthroline Ligand in Ionic Liquid. *Inorg. Chem.* **2020**, *59*, 3905–3911.
- (54) Ren, P.; Huang, P.-w.; Yang, X.-f.; Zou, Y.; Tao, W.-q.; Yang, S.-l.; Liu, Y.-h.; Wu, Q.-y.; Yuan, L.-y.; Chai, Z.-f.; Shi, W.-q. Hydrophilic Sulfonated 2,9-Diamide-1,10-phenanthroline Endowed with a Highly Effective Ligand for Separation of Americium(III) from Europium(III): Extraction, Spectroscopy, and Density Functional Theory Calculations. *Inorg. Chem.* **2021**, *60*, 357–365.
- (55) Zhang, X.; Kong, X.; Yuan, L.; Chai, Z.; Shi, W. Coordination of Eu(III) with 1,10-Phenanthroline-2,9-dicarboxamide Derivatives: A Combined Study by MS, TRLIF, and DFT. *Inorg. Chem.* **2019**, *58*, 10239–10247.
- (56) Afsar, A.; Laventine, D. M.; Harwood, L. M.; Hudson, M. J.; Geist, A. Utilizing electronic effects in the modulation of BTPhen ligands with respect to the partitioning of minor actinides from lanthanides. *Chem. Commun.* **2013**, *49*, 8534–8536.
- (57) Zhang, A.; Xu, L.; Lei, G. Separation and complexation of palladium(ii) with a new soft N-donor ligand 6,6'-bis(*S,S*-dinonyl-1,2,4-triazin-3-yl)-2,2'-bipyridine (C9-BTBP) in nitric acid medium. *New J. Chem.* **2016**, *40*, 6374–6383.
- (58) Fang, Y.; Yuan, X.; Wu, L.; Peng, Z.; Feng, W.; Liu, N.; Xu, D.; Li, S.; Sengupta, A.; Mohapatra, P. K.; Yuan, L. Ditopic CMPO-pillar[*S*]arenes as unique receptors for efficient separation of americium(iii) and europium(iii). *Chem. Commun.* **2015**, *51*, 4263–4266.
- (59) Wu, Q.-Y.; Wang, C.-Z.; Lan, J.-H.; Xiao, C.-L.; Wang, X.-K.; Zhao, Y.-L.; Chai, Z.-F.; Shi, W.-Q. Theoretical Investigation on Multiple Bonds in Terminal Actinide Nitride Complexes. *Inorg. Chem.* **2014**, *53*, 9607–9614.
- (60) Wu, Q.-Y.; Song, Y.-T.; Ji, L.; Wang, C.-Z.; Chai, Z.-F.; Shi, W.-Q. Theoretically unraveling the separation of Am(III)/Eu(III): insights from mixed N,O-donor ligands with variations of central heterocyclic moieties. *Phys. Chem. Chem. Phys.* **2017**, *19*, 26969–26979.
- (61) Kong, X.-H.; Wu, Q.-Y.; Lan, J.-H.; Wang, C.-Z.; Chai, Z.-F.; Nie, C.-M.; Shi, W.-Q. Theoretical Insights into Preorganized Pyridylpyrazole-Based Ligands toward the Separation of Am(III)/Eu(III). *Inorg. Chem.* **2018**, *57*, 14810–14820.